

# Microwave deicing performance and low-temperature cracking resistance evaluation of asphalt mixture incorporating graphene-coated functional aggregates

Shaowei Zhang

*Department of Civil and Environmental Engineering, The Hong Kong Polytechnic University, Hong Kong Special Administrative Region.*

Zhen Leng\*

*Department of Civil and Environmental Engineering, The Hong Kong Polytechnic University, Hong Kong Special Administrative Region.*

**ABSTRACT:** Ice/snow on pavements is a constant threat to traffic safety and needs to be removed efficiently. Graphene as novel carbon nanomaterial have excellent microwave-absorbing and mechanical properties, making it the most favorable candidate for heating-generation composites. But there is a problem of uneven dispersion when introducing them through traditional processes. This research aims to fabricate graphene-coated functional aggregate (FLG@FA) to boost pavement deicing via a new coating method and high-temperature curing process. Microwave deicing and Low-temperature semi-circular bending (SCB) test at a low load-line displacement (LLD) rate were conducted to evaluate the ice-melting and low-temperature performance. Results show that deicing velocity of FLG@FA could be enhanced to 29.6 g/min (~64%↑). It also demonstrated an enhanced level of low-temperature cracking resistance (~31.4%↑) evaluated by calculating modified fracture work ( $W_f$ ).

## 1 INTRODUCTION

Ice/snow on transportation infrastructure is a constant threat to traffic safety and needs to be removed efficiently to maintain normal operations (Sun et al., 2012). There are multiple deicing approaches, such as removal techniques, ice-melting chemicals, the hydronic pipe method, and self-healing technology (Qiu and Nixon, 2008). Among them, chemical agents like salt and mechanical means have been most prevalently utilized. Nevertheless, the overuse of salt commonly results in environmental pollution and corrosion issues. Meanwhile, removal methods exhibit low work efficiency and are liable to cause damage to the pavement surface. The hydronic pipe method is also favored, but its application is relatively costly and complex, which alters the internal pavement structure and poses potential risks to durability. Thus, it is of great significance to investigate efficient and eco-friendly ice-melting technologies.

Nowadays, self-healing heating technology has become a research hotspot. It is closely related to the road surface temperature. Electromagnetic induction and microwave heating are used in self-healing technology, and microwave heating has more advantages like uniform heating and high efficiency (Wang et al., 2022). Scholars have conducted a large number of studies on microwave snow and ice-melting asphalt pavements. For example, Sun et al. studied the heating rate of steel fiber-modified asphalt pavements under microwave radiation (Sun et al., 2023). Arabzadeh et al. used carbon fiber-modified asphalt concrete for anti-icing and deicing (Arabzadeh et al., 2019). Gao et al. verified the fea-

sibility of steel slag for microwave deicing (Gao et al., 2017). Microwave deicing technology has advanced, but its use is restricted as current magnetic substitutes underperform in deicing, leading to low efficiency and weak competitiveness. Immediate material and technical upgrades are essential to enhance its practicality and competitiveness.

Nano-carbon materials like graphene have great abilities in absorbing electromagnetic waves and conductivity and also possess many excellent mechanical properties (Tan et al., 2023). Incorporating them into asphalt pavement can solve related limitations (Kim et al., 2015). However, nanomaterials are prone to form agglomerates due to the high van der Waals force among themselves, making it difficult for graphene to be effectively dispersed in a high-viscosity asphalt. Using nano-carbon materials as coating materials to prepare functional aggregates for microwave deicing can overcome the dispersion problem and improve the insufficient electromagnetic wave absorption ability. However, there is still a research gap regarding this deicing technology.

This research aims to fabricate the graphene-coated functional aggregates (FLG@FA) for improved deicing efficiency of asphalt pavement via a novel coating method. The microwave ice-melting performance of the FLG@FA group was investigated. Meanwhile, the evaluation of deicing asphalt mixture's low-temperature performance is of great significance for mitigating transverse thermal cracking and preventing traffic accidents. Low-temperature SCB tests at a slow load-line displacement (LLD) rate of 0.5 mm/min and an improved


calculation method of  $W_f$  will be conducted for the evaluation of low-temperature cracking resistance.

## 2 MATERIALS AND METHODOLOGY

### 2.1 Materials

Raw materials of few-layer graphene (FLG) dispersion and nanoceramic resin were selected to prepare the functional ink before coating. Well-dispersed functional ink (FLG ink) was synthesized by thorough shear mixing of FLG dispersion with ceramic resin using a dispersion disc and mixer at 1000 rpm for 30 min at ambient temperature. The fundamental properties of FLG ink are presented in Table 1. Raw granite aggregate (RA), the most commonly used aggregate in Hong Kong, and an asphalt binder with a performance grading (PG) from 76 to -22 °C, supplied by the local supplier, K. Wah Asphalt Limited, were selected.

Table 1. Fundamental properties of FLG ink.

Properties	FLG ink
Ingredients	FLG, isopropyl alcohol, ceramic resin, dispersing agents
Solid content	2.5%
State	Liquid
Color	Grey
Odor	Acetone-like
Density (25 °C)	1.08 g/cm <sup>3</sup>
Appearance	

### 2.2 Preparation of graphene-coated FA (FLG@FA)

The fabrication of FLG@FA was accomplished using FLG ink and RA, employing the flip-spraying technique and a high-temperature curing process. In the flip-spraying technique, FLG ink was applied to one surface of RA via a spray gun and an air pump. Subsequently, two foam pieces were utilized to sandwich the aggregates and then invert them, allowing for the application of FLG ink to the opposite side as well. This ensures a uniform coating of FLG ink over the aggregate's surface. During the curing process, FA with the ink on its surface, was initially left at room temperature for 30 minutes to facilitate the evaporation of the alcohol solvent. Subsequently, it was subjected to heating in an oven at 190 °C for an additional 30 minutes. This process allows for the formation of a functional film that adheres firmly to the aggregate surface. After the completion of the spraying and curing processes, FLG@FA, featuring a uniformly and firmly adhered FLG film on its surface, was successfully produced.

### 2.3 Preparation of specimens with FLG@FA

FLG@FA was used to prepare asphalt mixture specimens with PG 76/22 asphalt and filler. A porous asphalt mixture with a nominal maximum aggregate size of 13.2 mm (PA-13), an optimum asphalt-aggregate content of 4.1%, and a target void ratio of  $(20 \pm 0.5) \%$  were selected. The aggregates were preheated in an oven at 105 °C for more than 4 hours until reaching a constant weight and then further heated at 190 °C to ensure complete heating. Subsequently, they were mixed with hot asphalt binder heated at 170 °C following JTG E20-2011. It should be noted that after the heating procedures, the curing process of FA did not necessitate additional high-temperature treatment. After mixing and compacting, asphalt mixture specimens with RA or FLG@FA were obtained and three replicates of each type of specimen were tested.

### 2.4 Microwave deicing test

A microwave deicing test was conducted to evaluate the ice-melting efficiency. In this test, one standard Marshall specimen with RA or FLG@FA ( $\Phi 101.6$  mm  $\times$  63.5 mm) was used and an ice layer with a thickness of 10 mm was frozen on the surface (Figure 1). The 10 mm ice layer was prepared on the surface using a special mold with a 10 mm depth and the same inner diameter as the Marshall specimen. Those deicing specimens were initially maintained at a temperature of around -33 °C. Their melting performance was examined through microwave heating at a power of 800 W. The specimen was heated for 30 s and then allowed to rest for 10 s alternately. The intermission time within the heating intervals was employed to document the mass of the ice and the surface temperature of the ice layer under ambient temperature conditions (15 °C). The average ice-melting velocity ( $v$ ) was adopted to assess the melting efficiency, which is defined as follows:

$$v = \frac{m_2 - m_1}{t} \quad (1)$$

where  $m_1$  is the mass of test specimen before testing,  $m_2$  is the mass after testing, and  $t$  is the heating time.

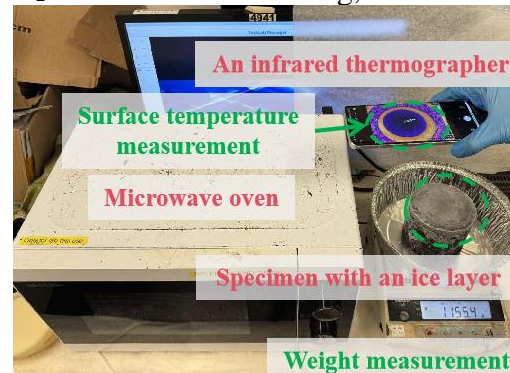


Figure 1. Experimental setup of ice-melting.

### 2.5 SCB test at lowPG+10 °C

SCB test is a well-established and practical method for assessing the cracking susceptibility of asphalt mixtures (Al-Qadi et al., 2015). The low-temperature cracking resistance was evaluated via the SCB test at a low temperature. Superpave gyratory compactor (SGC) specimens were shaped ( $\Phi 150 \text{ mm} \times 170 \text{ mm}$ ) and then sectioned into four semi-circular specimens ( $R150 \text{ mm} \times 50 \text{ mm}$ ). A notch ( $15 \text{ mm} \times 1.0 \text{ mm}$ ) was cut into the central bottom of each semi-circular specimen, aiming to ensure the cracking mode. Before testing, the specimens were subjected to a pre-conditioning treatment within a temperature-controlled chamber at a temperature of lowPG+10 (specifically  $-12 \text{ }^\circ\text{C}$ ) for a duration of 4 h using a DTS-30 universal testing machine. An LLD-controlled configuration facilitates a more accurate acquisition of the fracture energy, as its measurement aligns with the direction of load application (Son et al., 2019). Subsequently, the SCB test was executed at a slow LLD rate of  $0.5 \text{ mm/min}$ . Final analysis was performed by using the load-LLD curves and fracture energy ( $G_f$ ), which can be calculated using the following equation:

$$G_f = \frac{W_f}{A_{lig}} \quad (2)$$

$$A_{lig} = (r - l) \times t \quad (3)$$

$$W_f = \int_{u_0}^{u_p} P_1(u) du + \int_{u_p}^{u_f} P_2(u) du \quad (4)$$

where  $W_f$  is the fracture work (J);  $A_{lig}$  is the ligament area ( $\text{m}^2$ );  $r$  is the height of the specimen (mm),  $l$  is the depth of the notch (mm), and  $t$  is the thickness of the specimen (mm).

The flexibility index (FI), proposed by Ozer et al., serves as a crucial parameter for ascertaining the damage potential of asphalt mixture (Ozer et al., 2016). According to experimental results, differences were found between load-displacement curves under the low-temperature condition and typical outcomes of the SCB test. Specifically, the curve under low temperature exhibits unique patterns as shown in Figure 2. Compared with the typical curve (left), it is evident from the right curve that a pronounced and linear downtrend is observable immediately after attaining the peak load. This phenomenon can be attributed to the transformation of the asphalt mixture from a viscoelastic material to a completely brittle one under low temperatures. After reaching the peak load, specimens snapped suddenly. As this material property changed, the test controlled by The LLD mode proved inadequate in capturing the post-peak slope, a critical parameter for reliable FI calculation, thus preventing accurate de-

termination of the FI indicator. In addition, the area of the fracture work necessitated adjustment to the area of the curve ranging from the initial point ( $u_0$ ) to the point corresponding to the peak load ( $u_p$ ) since the specimen underwent brittle fracture after reaching the peak load. The modified calculation is shown as follows:

$$W_f = \int_{u_0}^{u_p} P(u) du \quad (5)$$

where  $u_0$  is the displacement at the contact load of  $0.1 \text{ kN}$  (mm) and  $u_p$  is the displacement at the peak load (mm).

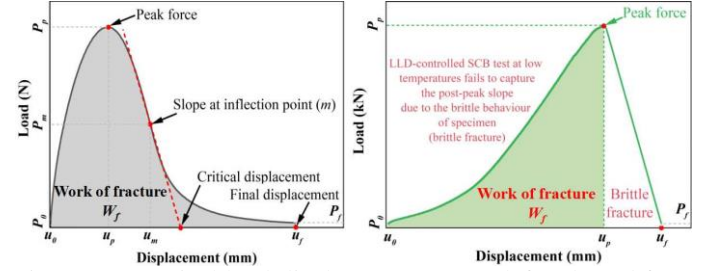


Figure 2. A typical load-displacement curve (left, adapted from (Al-Qadi et al., 2015)) and a load-displacement curve at lowPG+10 °C (right).

## 3 TEST RESULTS AND ANALYSIS

### 3.1 Microwave deicing behavior

Figure 3 presents the alterations in the average temperature of the ice surface on the specimen. The specimen with FLG@FA exhibits a considerably higher temperature increase rate compared to RA. FLG@FA curtailed the time of three microwave heating cycles (i.e., 90 s) to melt an ice layer with a thickness of 10 mm at an initial temperature of around  $-33 \text{ }^\circ\text{C}$ . After 150 s of microwave heating, the ice layer was entirely melted, and the average surface temperature of the ice layer reached  $32.1 \text{ }^\circ\text{C}$ , which is higher than that of RA ( $30.2 \text{ }^\circ\text{C}$ ). Notably, RA demanded a longer heating duration of 240 s. Despite the complete melting, the extended time implies that the ice absorbs and transforms microwave energy into heat inefficiently, thereby emphasizing the feeble responsiveness to microwave heating. As depicted in Figure 4, FLG@FA attained an ice-melting velocity of  $29.6 \text{ g/min}$  (an enhancement of  $\sim 64\%$ ) in comparison to RA ( $18.1 \text{ g/min}$ ) for melting the ice layer, thus manifesting the remarkable microwave deicing capacity of FLG@FA.

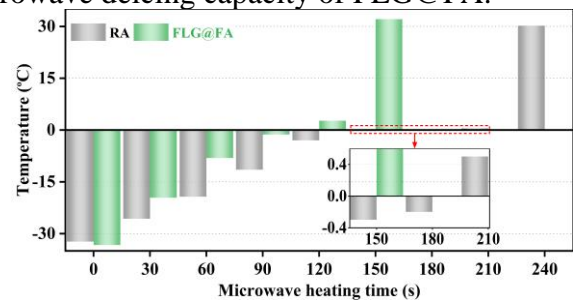


Figure 3. The average surface temperature on the ice layer.



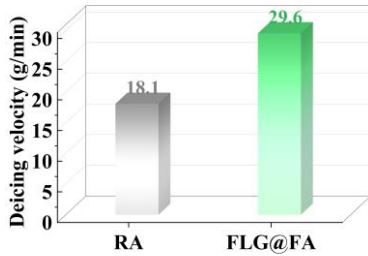


Figure 4. Deicing velocity results of specimens.

### 3.2 Low-temperature cracking resistance

The typical load-displacement curves and fracture energy of RA and FLG@FA group obtained from the low-temperature SCB test are illustrated in Figure 5. The low-temperature curves exhibit unique patterns as previously mentioned (left). A distinct and linear downward trend was discernible after reaching the peak load (brittle behavior). The load-displacement curve of FLG@FA exhibited a higher peak load of 6.4 kN in contrast to that of RA, which was 6.1 kN. Simultaneously, it is observable that the  $W_f$  of RA (depicted by the gray area) ranging from  $u_0$  to  $u_p$  is smaller than that of FLG@FA (green area). Subsequently, the  $G_f$  was determined by conducting integrations and calculations based on modified Equation 5 and Equation 2. The resultant values are illustrated in Figure 5 (right). Compared to the control group with a  $G_f$  value of 306.1 J/m<sup>2</sup>, FLG@FA augmented its  $G_f$  value to 402.2 J/m<sup>2</sup>, showing a substantially enhancing effect on low-temperature cracking resistance, with an improvement rate of approximately 31.4%.

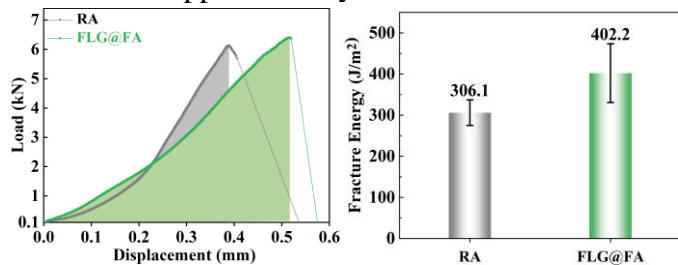


Figure 5. Typical load-displacement curve illustration for modified fracture work calculation (left) and fracture energy of SCB test at lowPG+10 °C (right) of RA and FLG@FA.

## 4 CONCLUSIONS

1. Functional aggregate firmly coated with graphene film on the surface can be prepared through the flip-spraying method and curing process.
2. FLG@FA demonstrated improvements in both microwave ice-melting performance and low-temperature cracking resistance: its ice-melting velocity at -33 °C increased by 64% from 18.1 g/min to 29.6 g/min for a 10 mm ice layer while cracking resistance evaluated by an improved fracture work calculation method showed a 31.4% enhancement compared to RA.

3. FLG@FA preliminary demonstrated the potential for microwave ice-melting on asphalt pavements. Comprehensive investigations are necessary and future research will focus on the evaluation of moisture susceptibility, mechanical performance, cost analysis, and other related aspects.

## REFERENCES

- AL-QADI, I. L., OZER, H., LAMBROS, J., KHATIB, A. E., SINGHVI, P., KHAN, T., RIVERA-PEREZ, J. & DOLL, B. 2015. Testing protocols to ensure performance of high asphalt binder replacement mixes using RAP and RAS.
- ARABZADEH, A., NOTANI, M. A., KAZEMIYAN ZADEH, A., NAHVI, A., SASSANI, A. & CEYLAN, H. 2019. Electrically conductive asphalt concrete: An alternative for automating the winter maintenance operations of transportation infrastructure. *Composites Part B: Engineering*, 173, 106985.
- GAO, J., SHA, A., WANG, Z., TONG, Z. & LIU, Z. 2017. Utilization of steel slag as aggregate in asphalt mixtures for microwave deicing. *Journal of Cleaner Production*, 152, 429-442.
- KIM, M. S., JANG, D. U., HONG, J. S. & KIM, T. 2015. Thermal modeling of railroad with installed snow melting system. *Cold Regions Science and Technology*, 109, 18-27.
- OZER, H., AL-QADI, I. L., SINGHVI, P., KHAN, T., RIVERA-PEREZ, J. & EL-KHATIB, A. 2016. Fracture Characterization of Asphalt Mixtures with High Recycled Content Using Illinois Semicircular Bending Test Method and Flexibility Index. *Transportation Research Record*, 2575, 130-137.
- QIU, L. & NIXON, W. 2008. Effects of Adverse Weather on Traffic Crashes: Systematic Review and Meta-Analysis. *Transportation Research Record Journal of the Transportation Research Board*, 2055, 139-146.
- SON, S., SAID, I. M. & AL-QADI, I. L. 2019. Fracture properties of asphalt concrete under various displacement conditions and temperatures. *Construction and Building Materials*, 222, 332-341.
- SUN, Y., ZHENG, L., CHENG, Y., CHI, F., LIU, K. & ZHU, T. 2023. Research on maintenance equipment and maintenance technology of steel fiber modified asphalt pavement with microwave heating. *Case Studies in Construction Materials*, 18, e01965.
- SUN, Z., MASA, J., LIU, Z., SCHUHMANN, W. & MUHLER, M. 2012. Highly concentrated aqueous dispersions of graphene exfoliated by sodium taurodeoxycholate: dispersion behavior and potential application as a catalyst support for the oxygen-reduction reaction. *Chemistry—A European Journal*, 18, 6972-6978.
- TAN, Y., WANG, W., XU, Y., XING, C., LIANG, Z. & ZHANG, J. 2023. Investigation on preparation and properties of carbon fiber graphite tailings conductive asphalt mixture: A new approach of graphite tailings application. *Construction and Building Materials*, 402, 133057.
- WANG, F., ZHU, H., SHU, B., LI, Y., GU, D., GAO, Y., CHEN, A., FENG, J., WU, S., LIU, Q. & LI, C. 2022. Microwave heating mechanism and self-healing performance of asphalt mixture with basalt and limestone aggregates. *Construction and Building Materials*, 342, 127973.